

## Supporting Information

### Oxalate-Assisted Formation of Uniform Carbon-Confined SnO<sub>2</sub> Nanotubes with Enhanced Lithium Storage

Chunhua Han,<sup>a</sup> Baoxuan Zhang,<sup>a</sup> Kangning Zhao,<sup>a</sup> Jiashen Meng,<sup>a</sup> Qiu He,<sup>a</sup> Pan He,<sup>a</sup>  
Wei Yang,<sup>a</sup> Qi Li<sup>a</sup> and Liqiang Mai<sup>\*ab</sup>

<sup>a</sup>State Key Laboratory of Advanced Technology for Materials Synthesis and  
Processing, Wuhan, 430070 Hubei, China

<sup>b</sup>Department of Chemistry, University of California, Berkeley, California 94720,  
United States. E-mail: mlq518@whut.edu.cn

#### Experimental

##### Synthesis of MnOOH nanowires

MnOOH nanowires were synthesized according to a reported hydrothermal method.<sup>1</sup> In a typical synthesis, 0.167 g of KMnO<sub>4</sub> and 3.33ml of polyethylene glycol (PEG400) were dissolved in 70 mL of deionized (DI) water with vigorous magnetic stirring at room temperature for 30 min, and then the resulting solution was transferred into a 100 mL Teflon-lined stainless-steel autoclave. The autoclave was sealed and maintained in an electric oven at 160 °C for 5 h. After cooling down to room temperature, the brown product was harvested by centrifugation, washed with DI water and ethanol several times, and dried at 70 °C overnight.

##### Synthesis of SnO<sub>2</sub> nanotubes

0.088 g of MnOOH nanowires were dispersed in 25 mL of deionized (DI) water and 20ml of ethanol by ultra-sonication for 30 min in a beaker. Then 0.189g of SnCl<sub>2</sub> dispersed in 10 ml of HCl solution (1.2M) and 0.202g of Na<sub>2</sub>C<sub>2</sub>O<sub>4</sub> dispersed in 10 mL of deionized (DI) water were added into the above suspension under constant magnetic stirring. After thorough mixing, the suspension was transferred into a water bath pot at 60 °C for 4 h. The white product was collected by several rinse-centrifugation cycles, and dried at 70 °C overnight.

##### Synthesis of SnO<sub>2</sub>@C nanotubes

A thin dopamine-derived carbon layer is uniformly coated on the surface of SnO<sub>2</sub> nanotubes using the reported method.<sup>2</sup> In a typical synthesis, 120 mg of SnO<sub>2</sub> nanotubes was first dispersed in 150

mL of trisbuffer solution (10 mM) under sonication for 10 min. Then, 60 mg of dopamine hydrochloride was added with vigorous stirring for 6 h. The resulting precipitate was collected by centrifugation, washed several times by DI water and ethanol, and dried at 70 °C overnight. The as-synthesized SnO<sub>2</sub>@PDA nanotubes were first carbonized at 500 °C for 4 h under a nitrogen atmosphere with a heating rate of 5 °C min<sup>-1</sup>. Finally, the carbon-coated SnO<sub>2</sub> nanotubes were collected by repeated rinse-centrifugation cycles with DI water and ethanol, and dried at 70 °C overnight.

### **Characterizations**

X-ray diffraction (XRD) patterns were determined on a Bruker D8 Advance X-ray diffractometer with Cu K $\alpha$  radiation ( $\lambda = 1.5406 \text{ \AA}$ ). Scanning electron microscopy (SEM) images were taken using a JEOL JSM-7100F microscope. Transmission electron microscopy (TEM) images were acquired on a JEOL JEM-2100F STEM/EDS microscope. Thermogravimetric analysis (TGA) was performed using a Netzsch STA 449C simultaneous analyzer under an air flow with a temperature ramp of 10 °C min<sup>-1</sup>. The Brunauer–Emmett–Teller (BET) specific surface area was analyzed using a Micromeritics Tristar 3020 instrument at 77K. Raman spectra were obtained using a Renishaw INVIA micro-Raman spectroscopy system.

### **Electrochemical measurements**

The electrochemical measurements were carried out using CR2016 coin cells. The working electrode was composed of an active material, carbon black, and aqueous binder (Sodium alginate) with a weight ratio of 6:3:1. Lithium discs were employed as both counter electrode and reference electrode. The electrolyte is 1 M LiPF<sub>6</sub> in a mixture of ethylene carbonate, diethyl carbonate and ethyl methyl carbonate (1:1:1 by weight). The coin cells were assembled in an argon-filled glovebox with moisture and oxygen concentrations below 1.0 ppm. The charge–discharge measurements were galvanostatically performed on a NEWARE battery tester. Cyclic voltammetry (CV) tests were carried out on a CHI 760D electrochemical workstation. CV was measured at a scan rate of 0.1 mV s<sup>-1</sup>. Electrochemical impedance spectroscopy (EIS) was carried out using an Autolab PGSTAT 302N electrochemical workstation. EIS was achieved by applying a sine wave with an amplitude of 10.0 mV over the frequency range of 10 kHz to 0.1 Hz.

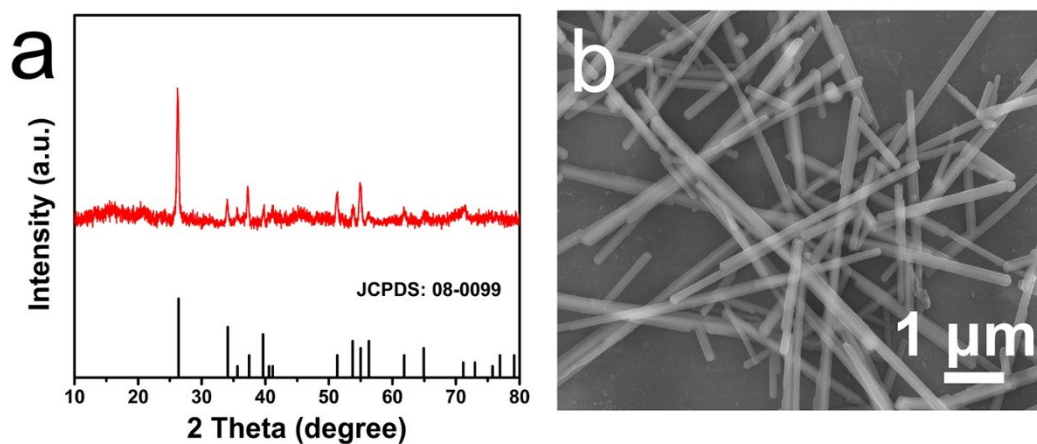


**Fig. S1** (a) XRD pattern, (b) SEM of the product obtained without extra reductant.

**Tab. S1** Reduction potentials relative to the standard hydrogen electrode (SHE)

Reduction reaction	$E^\ominus$ (V vs SHE) <sup>a</sup>
$\text{MnOOH} + 3\text{H}^+ + \text{e}^- \rightarrow \text{Mn}^{2+} + 2\text{H}_2\text{O}$	1.650 V
$\text{O}_2 + 4\text{H}^+ + 4\text{e}^- \rightarrow 2\text{H}_2\text{O}$	1.229 V
$\text{Sn}^{4+} + 2\text{e}^- \rightarrow \text{Sn}^{2+}$	0.154 V
$2\text{CO}_2 + 2\text{e}^- \rightarrow \text{C}_2\text{O}_4^{2-}$	-0.595 V

<sup>a</sup>Reduction potentials given are for reactions in aqueous solutions at 25 °C.

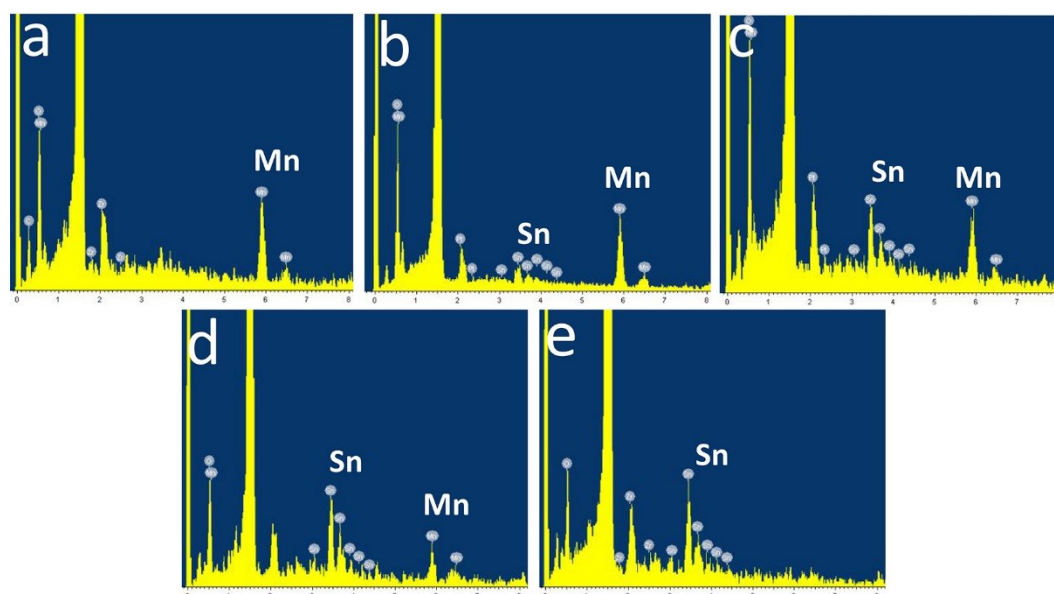


**Fig. S2** EDS spectra of the products at the reaction time of (a) 30 min, (b) 1 h, (c) 1.5 h, (d) 2 h, and (e) 3 h.

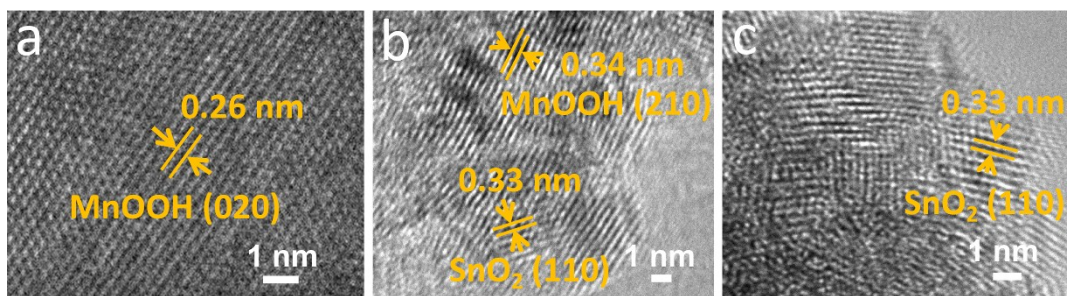


**Fig. S3** HRTEM images of (a) the initial product, (b) the intermediate product, (c) the final product.

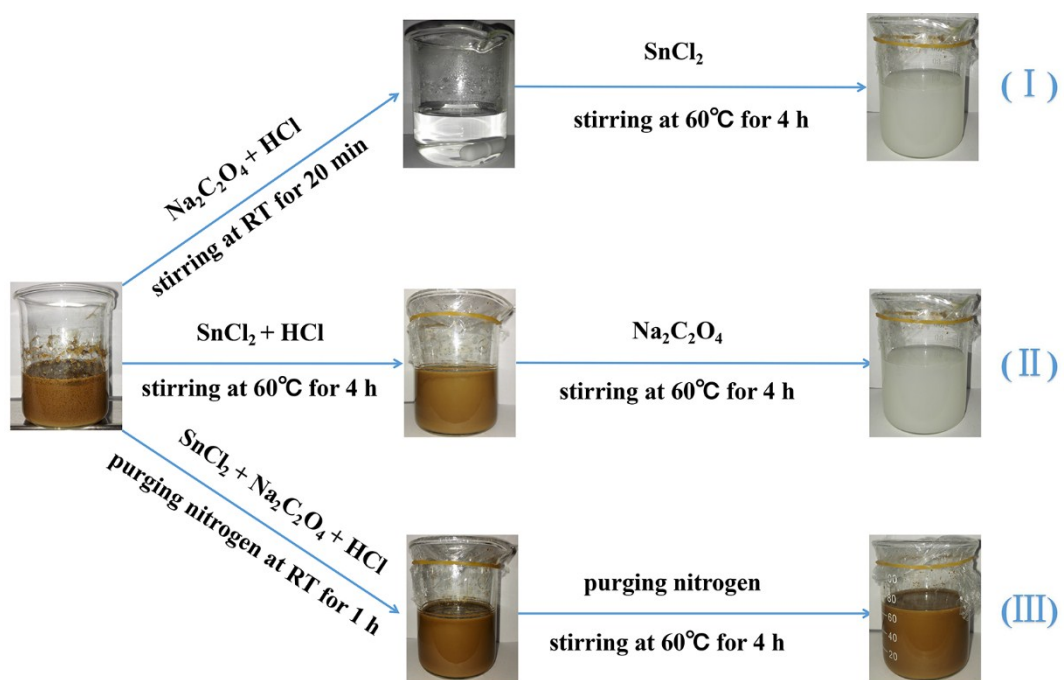


**Fig. S4** Schematic illustration of control experiments.

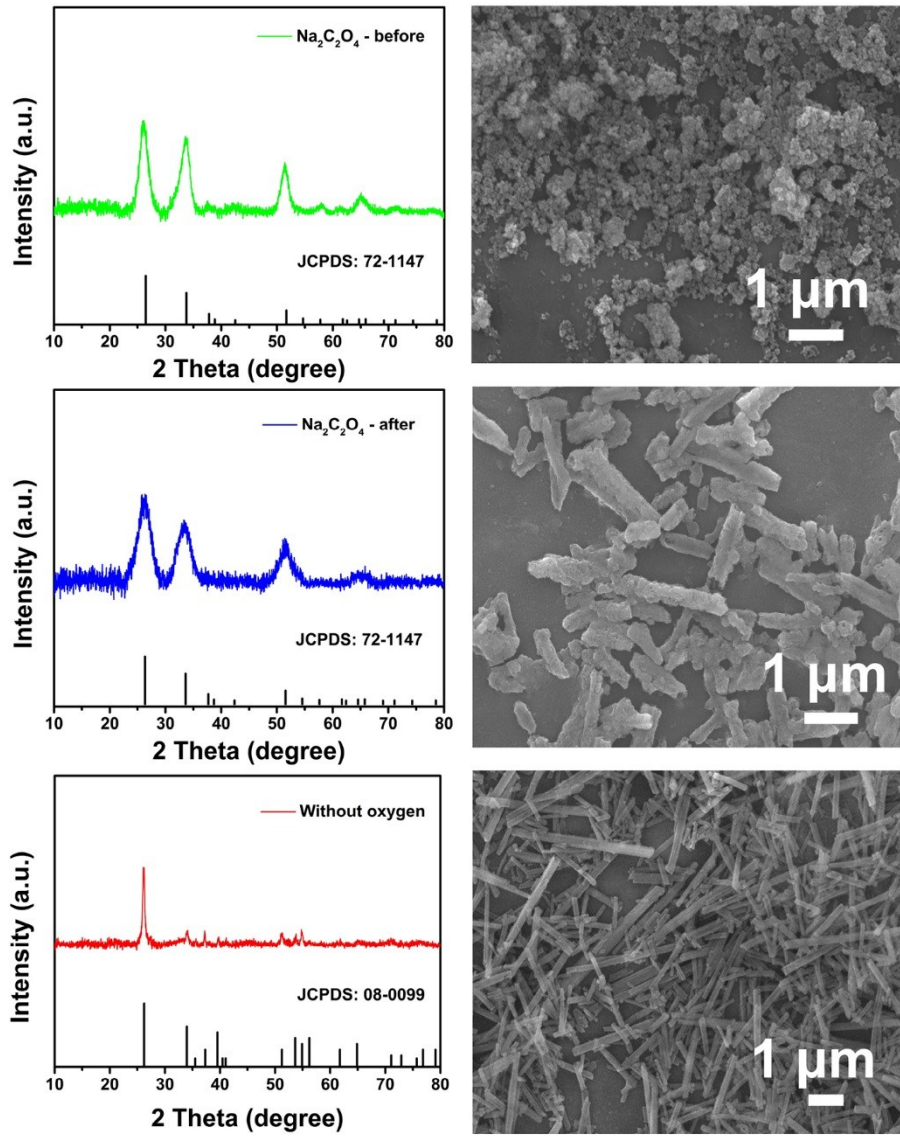


Fig. S5 (a) XRD pattern, (b) SEM image of  $\text{Na}_2\text{C}_2\text{O}_4$ -before; (c) XRD pattern, (d) SEM image of  $\text{Na}_2\text{C}_2\text{O}_4$ -after; (e) XRD pattern, (f) SEM image of the product under the condition of no oxygen.

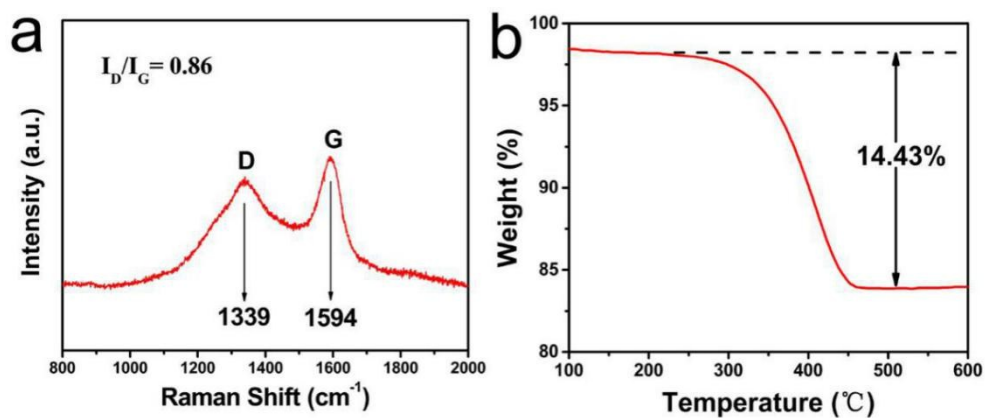
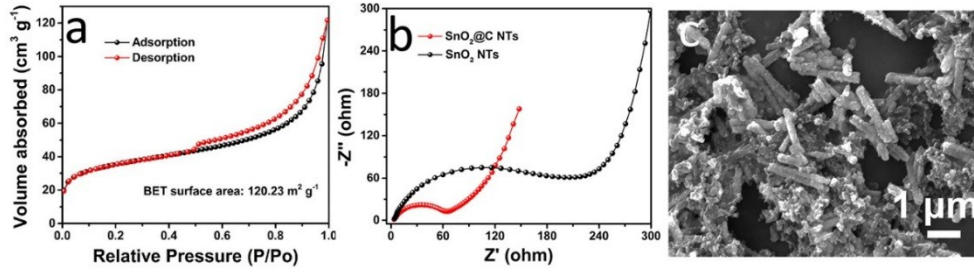


Fig. S6 (a) Raman spectrum, (c) TGA curve of  $\text{SnO}_2@\text{C}$  nanotubes.



**Fig. S7** (a)  $N_2$  adsorption-desorption isotherms of  $SnO_2$  nanotubes; (b) Nyquist plots of  $SnO_2@C$  nanotubes and  $SnO_2$  nanotubes; (c) SEM image of  $SnO_2@C$  nanotubes after cycling for 100 cycles under the current density of  $500 \text{ mA g}^{-1}$  within the potential range of  $0.01\sim 2.0 \text{ V}$ .

**Tab. S2** Rate capability of various  $SnO_2$ -based anode materials for lithium-ion batteries.

$SnO_2$ -based anode materials	Voltage range (V)	Current density ( $\text{mA g}^{-1}$ )	Discharge capacity ( $\text{mAh g}^{-1}$ )	Reference
$SnO_{2-x}$ : RGO	0.01~3	2000	700	3
$SnO_2/NC$ hNFs	0.01~3	2000	746	4
$SnO_2@G$ -SWCNT	0.01~3	2000	426	5
H- $SnO_2@rGO$	0.01~3	2000	546	6
graphene/ $SnO_2$	0.005 ~ 2.5	1000	492	7
PDA-coated $SnO_2$	0.01~3	2000	667	8
$SnO_2/C$ -NTs	0.01~2	2000	550	2
$SnO_2/NC$ submicroboxes	0.01~2	2000	499	9
C- $SnO_2/CNT$	0.01~ 2.5	4000	685	10
multi-shelled $SnO_2$ hollow microspheres	0.005 ~ 3	1000	436	11
$SnO_2$ -C composite	0.02 ~ 3	5000	510	12
$SnO_2$ QDs@GO	0.01~3	2000	566	13
Mo-doped $SnO_2$	0.01~3	1600	530	14
$SnO_2@DSC$	0.01~3	3000	462.5	15
hollow $SnO_2$ /polymer microsphere	0.01~ 2.5	4000	322	16
E- $SnO_2@C$	0.01~ 2.5	5000	755	17
core-shell $SnO_2$ - PANI nanorod arrays	0.005 ~ 2	3000	312	18
$CNT@SnO_2@C$	0.05 ~ 2.5	3600	590	19
$SnO_2@C$ nanotubes	0.01 ~ 2	2000	798	This work
		4000	711	

\*The values under the column of “Discharge capacity” are extracted from rate capacity curves.

## References

1. Z. Bai, B. Sun, N. Fan, Z. Ju, M. Li, L. Xu and Y. Qian, *Chem. Eur. J.*, 2012, **18**, 5319-5324.
2. X. Zhou, L. Yu and X. W. Lou, *Nanoscale*, 2016, **8**, 8384-8389.
3. W. Dong, J. Xu, C. Wang, Y. Lu, X. Liu, X. Wang, X. Yuan, Z. Wang, T. Lin, M. Sui, I. W. Chen and F. Huang, *Adv. Mater.*, 2017, **29**, 1700136.
4. D. Pham-Cong, J. S. Park, J. H. Kim, J. Kim, P. V. Braun, J. H. Choi, S. J. Kim, S. Y. Jeong and C. R. Cho, *Carbon*, 2017, **111**, 28-37.
5. J. Wang, F. Fang, T. Yuan, J. Yang, L. Chen, C. Yao, S. Zheng and D. Sun, *ACS Appl. Mater. Interfaces*, 2017, **9**, 3544-3553.
6. X. Hu, G. Zeng, J. Chen, C. Lu and Z. Wen, *J. Mater. Chem. A*, 2017, **5**, 4535-4542.
7. Q. Shao, J. Tang, Y. Sun, J. Li, K. Zhang, J. Yuan, D. M. Zhu and L. C. Qin, *Nanoscale*, 2017, **9**, 4439-4444.
8. B. Jiang, Y. He, B. Li, S. Zhao, S. Wang, Y. B. He and Z. Lin, *Angew. Chem. Int. Ed.*, 2017, **129**, 1869–1872.
9. X. Zhou, L. Yu and X. W. D. Lou, *Adv. Energy Mater.*, 2016, **6**, 1600451.
10. C. Ma, W. Zhang, Y. S. He, Q. Gong, H. Che and Z. F. Ma, *Nanoscale*, 2016, **8**, 4121-4126.
11. J. Zhang, H. Ren, J. Wang, J. Qi, R. Yu, D. Wang and Y. Liu, *J. Mater. Chem. A*, 2016, **4**, 17673-17677.
12. L. Shen, F. Liu, G. Chen, H. Zhou, Z. Le, H. B. Wu, G. Wang and Y. Lu, *J. Mater. Chem. A*, 2016, **4**, 18706-18710.
13. K. Zhao, L. Zhang, R. Xia, Y. Dong, W. Xu, C. Niu, L. He, M. Yan, L. Qu and L. Mai, *Small*, 2016, **12**, 588-594.
14. X. Wang, Z. Li, Z. Zhang, Q. Li, E. Guo, C. Wang and L. Yin, *Nanoscale*, 2015, **7**, 3604-3613.
15. Q. Tian, Y. Tian, Z. Zhang, L. Yang and S.-i. Hirano, *J. Mater. Chem. A*, 2015, **3**, 18036-18044.
16. M. Zhou, Y. Liu, J. Chen and X. Yang, *J. Mater. Chem. A*, 2015, **3**, 1068-1076.
17. A. Y. Kim, J. S. Kim, C. Hudaya, D. Xiao, D. Byun, L. Gu, X. Wei, Y. Yao, R. Yu and J. K. Lee, *Carbon*, 2015, **94**, 539-547.
18. W. Xu, K. Zhao, C. Niu, L. Zhang, Z. Cai, C. Han, L. He, T. Shen, M. Yan, L. Qu and L. Mai, *Nano Energy*, 2014, **8**, 196-204.
19. S. Chen, Y. Xin, Y. Zhou, F. Zhang, Y. Ma, H. Zhou and L. Qi, *J. Mater. Chem. A*, 2014, **2**, 15582.